



Cite this: *Environ. Sci.: Nano*, 2020, 7, 1633

Received 15th March 2020,
Accepted 10th May 2020

DOI: 10.1039/d0en00281j

rsc.li/es-nano

Ageing remarkably alters the toxicity of carbon black particles towards susceptible cells: determined by differential changes of surface oxygen groups†

Shuting Wei,^{‡abc} Yu Qi,^{‡bc} Li Ma,^d Yongchun Liu,^d Guangke Li,^a Nan Sang,^a Sijin Liu^{id} *^{bc} and Yajun Liu^{*e}

We uncover that O₃-induced ageing dynamically alters the surface O-functionalities of carbon black (CB) nanoparticles, a model of airborne particles. The consequent distinct bioreactivity and toxicity towards susceptible cells under low-dose exposure are largely attributed to the variant species of O-functionalities, thereby signifying the importance of the environmental ageing process in changing CB toxicity features.

Particulate matter (PM) pollution has become a highly concerning environmental problem, and results in severe health effects.^{1–3} After emission into the atmosphere, PMs will undergo atmospheric ageing in response to trace gases, such as SO₂, O₃, NO_x and so on.^{4–6} The ageing process not only affects the fate and transport of PMs, but also alters their physicochemical properties, *e.g.* morphologies, optical properties, surface functionalities and microstructures.^{7,8} For example, it has been documented that the ozonation of PMs increases the surface O-content and O-containing species including carbonyls and esters,⁹ and oxidation by H₂SO₄ gives rise to changes in the morphology of PMs.¹⁰ To this end, it would be plausible to suspect consequent variation of the toxicity of PMs post-ageing. However, despite adequate research interest in the ageing process, little understanding of the ageing-determined toxicity changes of PMs has been

Environmental significance

After emission, pristine air particles are subjected to significant attack under different atmospheric conditions, such as profound ageing upon interaction with trace gases including SO₂, O₃ and NO_x, giving rise to remarkable alterations in physicochemical properties. Despite numerous toxicity studies on fine air particles, rather limited knowledge has been obtained to interrogate ageing-determined toxicity changes. In the current study, we uncover that the O₃-induced ageing process renders remarkable alterations of the surface functional groups on carbon black (CB) particles, a model of fine air particles, resulting in reinforced bioreactivity towards two types of susceptible cells, namely erythroid cells and macrophages. Mechanistically, it is believed that the increase of O-containing groups, including epoxy, hydroxyl and carboxyl, putatively accounts for the increase in bioreactivity and resultant cytotoxicity. Moreover, the balance of epoxy and carboxyl groups fundamentally determines the toxic extent of aged CB particles. Collectively, this study unearths the significance of ageing in altering particle toxicity, and pinpoints the importance of defining detailed functional groups for toxicity assessment.

obtained. The most pronounced limitations are the influence of the complex atmospheric environment (*e.g.* sunlight,^{11,12} reactive gases,¹³ humidity,¹⁴ *etc.*) and the intricate components on PMs,^{15,16} which bring about considerable difficulties in differentiating the contributions of each variable. To circumvent this issue, a particle model has to be employed to tease out the mechanisms underlying ageing-associated toxicity changes. Carbon black (CB) particles, as a product of the incomplete combustion of heavy petroleum materials with a constant mass of pure elemental carbon (nearly 97%) and with a similar structure to the elemental carbon (EC) of PMs, represent an ideal model for this purpose.^{17–22}

It has been demonstrated that nano-sized particles (*i.e.* nano-sized PMs and synthesized nanoparticles, NP) could pass through the air–blood barrier to rapidly enter circulation once inhaled into the respiratory system, especially deep in the lungs.²³ Upon direct contact with various cells in circulation and eventually in distant tissues, a few types of

^a College of Environment and Resource, Research Center of Environment and Health, Shanxi University, Taiyuan, Shanxi, 030006, China

^b State Key Laboratory of Environmental Chemistry and Ecotoxicology, Research Center for Eco-Environmental Sciences, Chinese Academy of Sciences, Beijing, 100085, China. E-mail: sjliu@rcees.ac.cn

^c University of Chinese Academy of Sciences, Beijing, 100049, China

^d Aerosol and Haze Laboratory, Advanced Innovation Center for Soft Matter Science and Engineering, Beijing University of Chemical Technology, Beijing, 100029, China

^e Beijing Jishuitan Hospital, Peking University Health Science Center, Beijing, 100035, China. E-mail: drliuyajun@163.com

† Electronic supplementary information (ESI) available: The experimental section, Figures S1–S4 and Table S1 are provided in the ESI. See DOI: 10.1039/d0en00281j

‡ These authors contributed equally to this work.

cell stand out as playing an important role in particle transport and clearance. Red blood cells (RBCs) undoubtedly account for the delivery of particles to different organs through the bloodstream, and meanwhile macrophages build up the first line of defense against foreign particles through phagocytosis and pro-inflammatory responses.^{24–29} In this context, RBCs and macrophages represent crucial susceptible cell types in response to particle intrusion. As documented by previous studies, the *in vitro* and *in vivo* cytotoxicity of carbon-based NPs is mostly ascribed to their ability to kindle reactive oxygen species (ROS) generation, which may further induce DNA and mitochondrial damage, inflammation and even apoptosis.^{30–32} Notably, a largely overlooked aspect is using unrealistic exposure scenarios without considering environmental transformation and ageing. Under this setting, the influence of the ageing process on nano-sized PMs towards susceptible cells still remains elusive.

The primary objective of the current study is to interrogate whether CB particles are prone to changes in physicochemical properties when subjected to ageing induced by O₃, and to ask how the ageing process would change the toxicity profiles of CB towards susceptible cells under low-dose exposure scenarios with adequate environmental relevance. Collectively, our combined findings unearth the remarkable impact of ageing on CB physicochemical properties, leading to remarkably altered cytotoxicity profiles of CB particles towards susceptible cells including erythroid cells and macrophages upon low-dose exposure. The resultant cytotoxicity changes were dependent not only on the ozonation time, but also on variations of the surface functional groups. Moreover, the alteration of O-containing groups greatly retarded erythroid differentiation.

To mimic the ageing process in a real atmospheric environment, we exposed Printex U (abbreviated as PU) CB

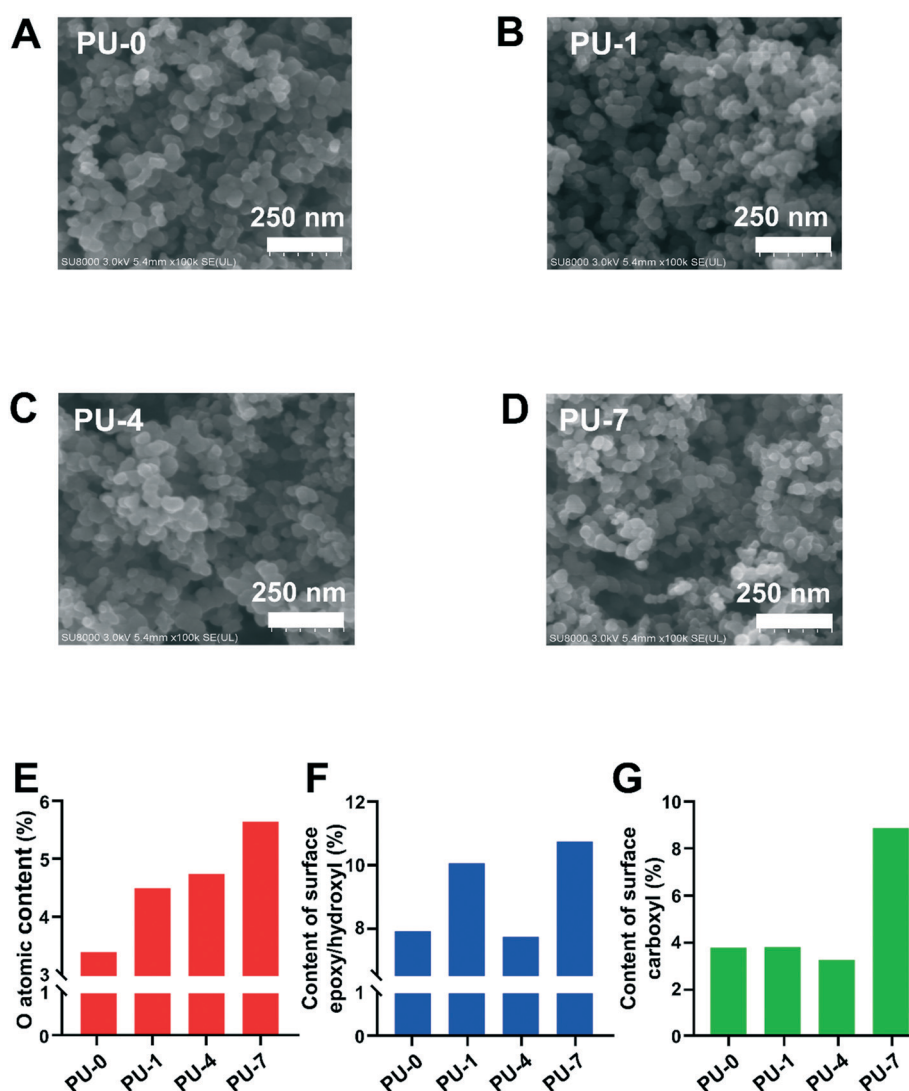


Fig. 1 Characterization of pristine and aged PU samples. (A–D) Representative SEM images of PU-0 (A), PU-1 (B), PU-4 (C) and PU-7 (D). (E) Quantification of O-content, surface epoxy/hydroxyl content (F) and surface carboxyl content (G) in PU-0, PU-1, PU-4 and PU-7, characterized by XPS spectra.

NPs to simulated air containing O₃ and ambient air. The O₃ concentrations used in these experiments corresponded to real O₃ levels in June 2018 in Beijing, China. Four exposure periods were conducted to simulate equivalent O₃ exposure for up to 7 days in the atmosphere, which were termed PU-0 (namely the parental or pristine condition), PU-1 (ageing for 1 day), PU-4 (ageing for 4 days) and PU-7 (ageing for 7 days). Scanning electron microscopy (SEM) images showed that the 3 groups of aged PU particles had a spherical shape with a diameter of around 20 nm, consistent with the parental PU (Fig. 1A–D), suggesting no significant change in morphological appearance post-ageing. Nonetheless, the hydrodynamic size exhibited marked variation after ageing, as the hydrodynamic size was calculated to be 220.4 nm for PU-0, 173.8 nm for PU-1, 164.5 nm for PU-4 and 140.9 nm for PU-7. This finding was consistently confirmed by the polydispersity index (PDI) and stability results (Table 1 and Fig. S1†). These observations therefore indicated that the colloidal stability of PU increased after ageing, with enhanced dispersibility and solubility. Moreover, in line with previous reports,³³ we found various metals in these PU samples, as determined by inductively coupled plasma mass spectrometry (ICP-MS) analysis (Fig. S2†).

Afterwards, surface chemical properties were characterized in detail by X-ray photoelectron spectroscopy (XPS). In agreement with previous reports,³⁴ a considerable increase was found in the total surface O-content and various species of oxygen functional groups after different O₃ treatments (Table 1, Fig. 1E–G and Fig. S3†). As a result, the O/C ratio increased from 3.54% for pristine PU-0 to 4.75% for PU-1, 5.02% for PU-4, and 6.02% for PU-7 (Table 1, $P < 0.05$). In more detail, the content of epoxy/hydroxyl groups was elevated to 10.09% in PU-1 and 10.78% in PU-7, relative to the original PU-0 at 7.93%, but no increase was found in PU-4 (Fig. 1F). Moreover, in contrast to PU-1, PU-7 displayed a much higher content of carboxyl groups at 8.88% relative to 3.78%, 3.80% and 3.25% for PU-0, PU-1 and PU-4, respectively (Fig. 1G). Notably, carbonyl groups were detected only in PU-4 with approximately 1.88%, but not in the other 3 PU samples. These data thus revealed the dynamic oxidation formation of O-containing groups during ageing, presumably from epoxy/hydroxyl groups (C–O–C/C–OH) to carbonyl groups (C=O) and finally carboxyl groups (COOH).³⁵ Additionally, the surface charge of PU-0 in

deionized (DI) water slightly declined from –9.88 mV to –10.90 mV for PU-1, –11.10 mV for PU-4 and –11.30 mV for PU-7 (Table 1), putatively as a consequence of the increased surface O-content.¹⁸ Together, these changes in physicochemical properties revealed that the O₃-induced ageing process significantly transformed PU particles by differentially oxidizing surface functional groups depending on duration.

Since the cytotoxicity of carbonaceous particles is fundamentally determined by their surface chemical groups,^{36–39} we would assume that the transformation of PU particles would surely alter their cytotoxicity towards susceptible cells. To test this hypothesis, the cytotoxicity of aged PU in comparison to the parental PU was assessed in susceptible cells including erythroid cells and macrophages. First, we performed hemolysis experiments with parental and aged PU particles. To set up the system, fresh blood was drawn from male Balb/C mice, followed by washing with phosphate buffered saline (PBS). Thereafter, the collected RBCs were subjected to exposure to different PU particles at 10 μg mL⁻¹ for 6 h, and then the hemoglobin released in the supernatant due to RBC lysis was quantified spectroscopically by absorbance at 414 nm. As shown in Fig. 2A, PU-1 caused the most severe hemolysis, characterized by a more than 2.1-fold increase of the absorbance value at 414 nm; in contrast, only a 7% increase was observed in PU-0-treated RBCs compared to untreated cells (Fig. 2A, $P < 0.001$ for PU-1-treated cells relative to untreated cells and PU-0-treated cells). PU-4 and PU-7 also markedly induced hemolysis by approximately 50% relative to the untreated control and PU-0-treated cells ($P < 0.001$), but to a lesser extent than PU-1 ($P < 0.001$) (Fig. 2A). Further, representative photographs of the treated RBCs confirmed these differences (Fig. 2B). These observations thereby unveiled the increased bioreactivity of aged PU particles towards RBCs, especially PU-1.

To corroborate the above finding, erythroid cells were assayed upon treatment with different PU particles. A well-recognized mouse erythroleukemia (MEL) cell line was employed for this purpose. Consistent with the above observations, overall aged PU particles revealed greater cytotoxicity in MEL cells. As shown in Fig. 2C, all 4 types of PU particles exhibited dose-dependent cytotoxicity in MEL cells, and aged particles showed enhanced cytotoxicity in MEL cells relative to the pristine particles. Of the aged PU

Table 1 Representative physicochemical properties of parental PU and aged PU particles

Parental PU/aged PU ^a	C ^b (wt%)					Total O ^b (wt%)	O/C ratio (%)	D _h ^c (nm)	PDI ^c	ζ potential (mV)
	Aromatic rings	Epoxy/hydroxyl	Carbonyl	Carboxyl	Total C ^b (wt%)					
PU-0	84.86	7.93	—	3.78	96.57	3.42	3.54	220.4 ± 3.2	0.201	–9.88 ± 0.97
PU-1	81.56	10.09	—	3.80	95.46	4.53	4.75	173.8 ± 2.3 ^d	0.135	–10.90 ± 0.17 ^d
PU-4	82.31	7.75	1.88	3.25	95.20	4.78	5.02	164.5 ± 4.9 ^d	0.092	–11.10 ± 0.20 ^d
PU-7	74.66	10.78	—	8.88	94.32	5.68	6.02	140.9 ± 0.5 ^d	0.077	–11.30 ± 0.35 ^d

^a Aged PU denotes PU-1, PU-4 and PU-7. ^b Determined by XPS. ^c D_h indicates the hydrodynamic diameter on the basis of particle size distribution analysis, and PDI represents the polydispersity index. ^d Statistical significance is defined as $P < 0.001$, compared to PU-0.

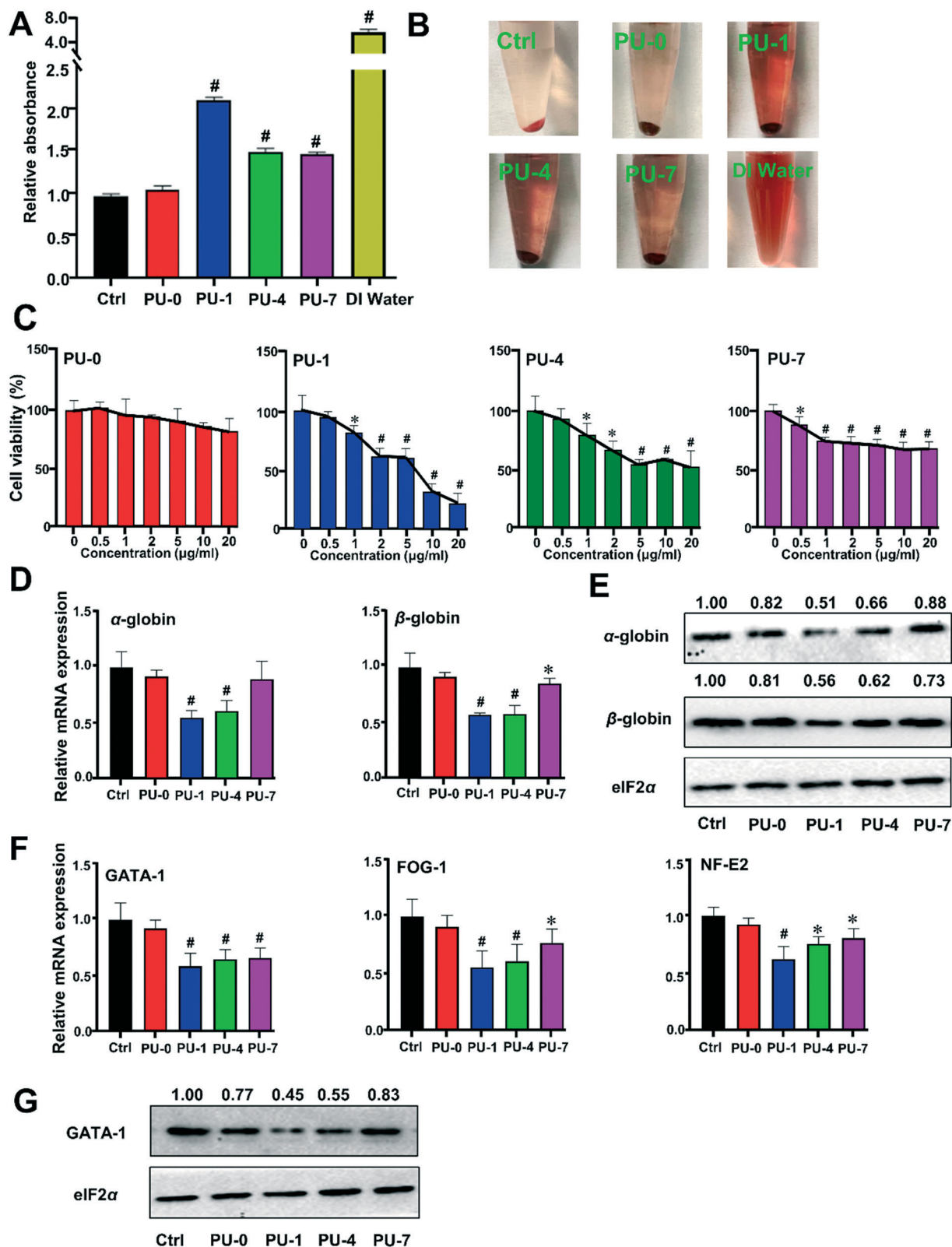


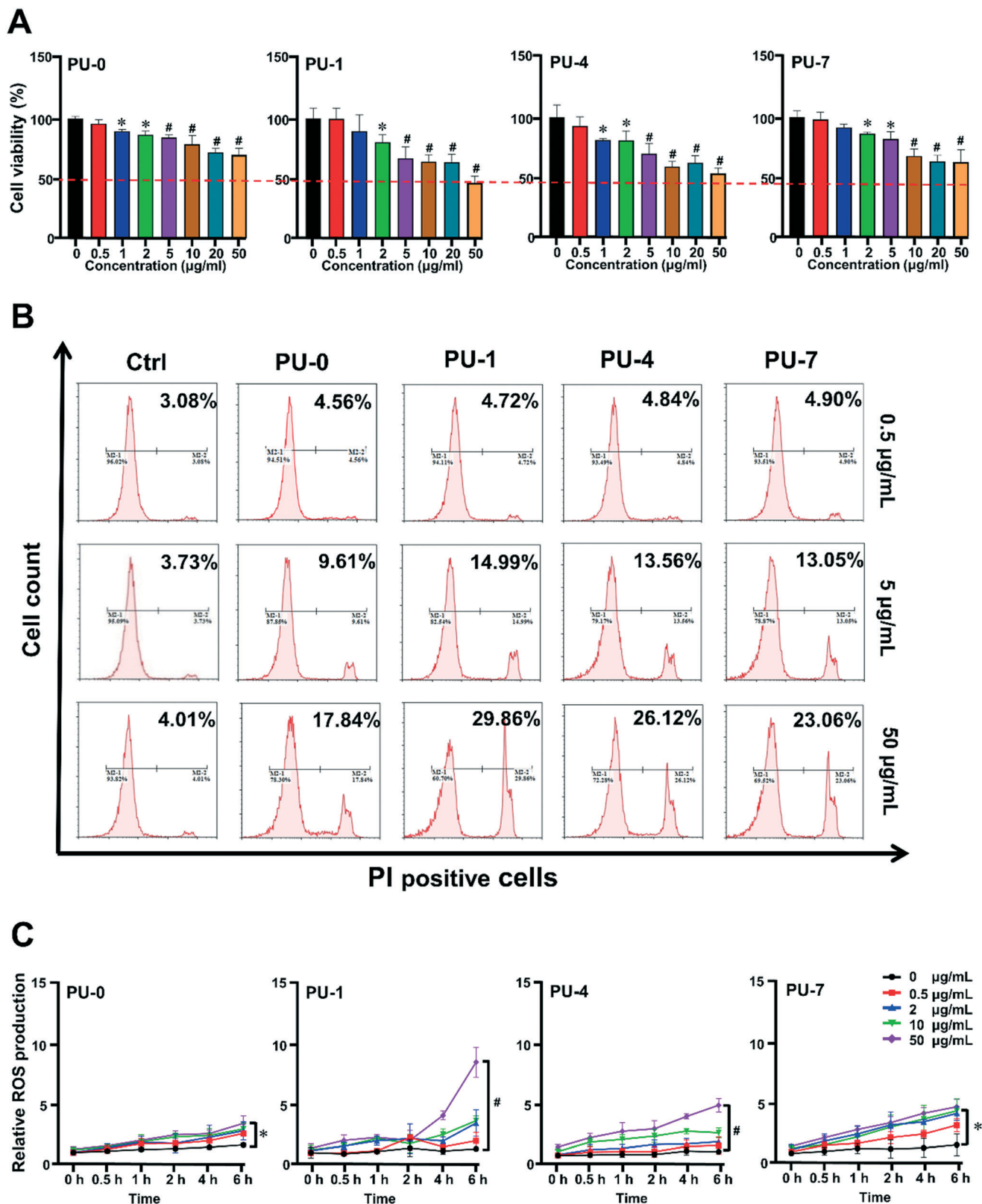
Fig. 2 Determination of hemolysis and cytotoxicity of pristine and aged PU samples in erythroid cells. (A) Relative quantification of hemolysis data of PU particles in RBCs at $10 \mu\text{g mL}^{-1}$ for 6 h. (B) Representative pictures of lysed RBCs in different groups. DI water was used as a positive control. (C) Cytotoxicity of different PU materials in MEL cells after 24 h treatment at various concentrations. (D) Gene expression levels, as reflected by RT-qPCR, and (E) protein concentrations of hemoglobins, as evidenced by Western blotting analysis, in DMSO-induced MEL cells after PU treatment at $1 \mu\text{g mL}^{-1}$ for 72 h. (F) Erythroid differentiation-related genes were determined by RT-qPCR analysis, and (G) the protein mass of GATA-1 was assessed by Western blotting in DMSO-induced MEL cells simultaneously upon PU treatment at $1 \mu\text{g mL}^{-1}$ for 72 h. Data are shown as mean \pm SD ($n = 3-5$). Statistical significance is defined as (*) $P < 0.05$ and (#) $P < 0.001$, compared to untreated cells.

samples, the greatest cytotoxicity was observed in PU-1-treated MEL cells, with 77% reduction of cell viability at 20 $\mu\text{g mL}^{-1}$ relative to the untreated cells, as evidenced by the cytotoxicity assay (Fig. 2C, $P < 0.001$). Milder cytotoxicity was demonstrated in PU-4- and PU-7-treated MEL cells, with 47% and 32% reduction of cell viability at 20 $\mu\text{g mL}^{-1}$, respectively, compared to the untreated control (Fig. 2C, $P < 0.001$). In support of our data, previous reports also documented increased toxicity of carbon-based particles after oxygenation.^{18,40}

Given the greatly changed bioreactivity of aged PU to erythroid cells, these results pinpointed the potential detrimental influence on erythroid cell differentiation and maturation. In the following, erythroid differentiation was examined by inducing MEL cell differentiation to mature RBCs by 1.5% dimethyl sulfoxide (DMSO), together with concurrent exposure to different PU particles.⁴¹ To avoid dramatic cell death, we deliberately used a low exposure dose, namely 1 $\mu\text{g mL}^{-1}$, where only a slight reduction of cell viability was visualized (Fig. 2C). To recognize erythroid differentiation, the mass of α -globin and β -globin expression was investigated according to a well-established method.⁴¹ As shown in Fig. 2D, the aged PU particles all reduced the expression of α -globin and β -globin after 72 h exposure, with the greatest reduction in PU-1-treated cells (with an approximately 50% drop relative to the untreated cells) ($P < 0.001$). In contrast, pristine PU-0 particles elicited mild repression of α -globin and β -globin expression compared to untreated cells (Fig. 2D). To substantiate this result, Western blotting analysis was conducted to verify the changes at the protein level. As shown in Fig. 2E, similar changes of α -globin and β -globin were demonstrated at the protein level, supporting the findings of impaired erythroid differentiation and maturation of MEL cells upon exposure to aged PU particles, in particular PU-1. To figure out the molecular processes dictating the impairment of erythropoiesis upon exposure to aged PU particles, the crucial signaling pathways in driving erythropoiesis, such as GATA-1/FOG-1 signaling and NF-E2 signaling,^{42–46} were closely probed. Fig. 2F shows a significant drop of GATA-1, FOG-1 and NF-E2 in aged PU-treated cells, in contrast to little change in the PU-0-treated cells compared to those in the control group ($P < 0.001$). Analogous to the above data, PU-1 elicited greater inhibition of the expression of these differentiation-related genes than PU-4 and PU-7. For example, PU-1 inhibited the expression of GATA-1 by 41% compared to the untreated cells ($P < 0.001$), while PU-4 and PU-7 caused a 35% and 34% decrease, respectively (Fig. 2F, $P < 0.001$). Analogously, Western blotting data confirmed the changes of GATA-1 protein in DMSO-induced MEL cells upon exposure to these PU particles (Fig. 2G). Considering these findings, ageing endows PU particles with even greater bioreactivity and more toxicity towards erythroid cells relative to pristine particles, highlighting the significance of ageing in transforming PU particles. These findings also underscore the distinct toxicity profiles of differentially aged PU particles.

In an effort to substantiate the above scientific statement, another susceptible cell model, RAW264.7 macrophage, was used to scrutinize the differential toxicity profiles responding to aged PU versus parental PU. In parallel to the findings in erythroid cells, as described in Fig. 3A, overall PU particles caused a reduction in the cell viability of RAW264.7 cells in a dose-dependent manner for PU-0, PU-1, PU-4 and PU-7 ($P < 0.05$). PU-1 was revealed to have the greatest toxicity, in contrast to PU-7, which showed much milder toxicity ($P < 0.05$). To be specific, the viability of RAW264.7 cells was reduced by 54% upon 50 $\mu\text{g mL}^{-1}$ PU-1 treatment, in contrast to 37% in PU-7-treated cells at the same concentration ($P < 0.05$). To validate these results, flow cytometry analysis was carried out to define the proportion of dead cells after propidium iodide (PI) staining. Similar results were found from flow cytometry data (Fig. 3B), corroborating the differential toxicities induced by different PU particles. Next, we sought to inspect the molecular mechanisms underlying these differential toxicity profiles in macrophages. To evidence the mitochondrial changes, we thoroughly surveyed the ROS production, as massive ROS production functions as an important hallmark of mitochondrial activity and injuries responding to endogenous or exotic stimuli.⁴⁷ Nevertheless, ROS induction would be a plausible mechanism to explain the adverse effects of inhaled particles.^{48,49} ROS generation was assayed in RAW264.7 cells upon PU treatment. As shown in Fig. 3C, only PU-1 provoked remarkable ROS generation, especially at high concentrations, and a slight induction of ROS was observed in PU-4- and PU-7-treated cells, compared to PU-0-treated cells. In support of our data, previous research also demonstrated that increased oxygen content, in particular epoxy groups and hydroxyl groups, confers on PU particles greater capability to provoke ROS and consequently oxidative stress.¹⁹ These ROS data further provided mechanistic insights into the differential toxicity profiles of distinctly aged PU particles. Furthermore, γ -H2AX, a cardinal indicator of DNA damage,⁵⁰ was assessed by Western blot analysis. The induction of γ -H2AX manifested a constant pattern of alteration, as the most abundant mass was observed in cells upon PU-1 treatment, followed by PU-4 treatment (Fig. S4†). These results of DNA injuries further supported our findings of the differential toxicity of aged PU particles.

In endeavoring to elucidate the physicochemical determinants of the enhanced cytotoxicity of aged PU particles, we surveyed the contribution of each parameter by comparison with the current literature. In line with previous studies,^{39,51,52} the oxygenation of CB particles greatly elevated their toxicity in various cells because of stability improvement, oxidative potential elevation, and the increase in O-containing groups (such as epoxy and hydroxyl).⁵³ Based on our results, a trend of cytotoxicity in RBCs, MEL erythroid cells and RAW264.7 macrophages could be determined, namely PU-0 < PU-7 < PU-4 < PU-1; however, this trend was not obviously correlated with a single surface variable. Given that no significant changes were observed in the morphology,



size and zeta potential, we thus focused on other important variables, *i.e.* the changes in surface functional groups upon O₃-induced ageing. Since the existence of epoxy groups is believed to be the most important determinant in causing toxicity,¹⁹ it should be assumed that PU-1 and PU-7 were similarly toxic to cells based on the above assumptions. Nevertheless, PU-1 was the most toxic, and PU-7 was the least toxic, suggesting that more variables were intertwined to account for the net toxicity. As shown in Table 1 and Fig. S2,† the hydrodynamic diameter of PU-7 was strikingly smaller than that of the other aged PU groups, suggesting that PU-7 exhibited better colloidal stability, with enhanced hydrophilicity and cytocompatibility, due to having the highest oxygen content and the most carboxyl groups on the surface. Thus, the distinct distribution pattern of epoxy/hydroxyl and carboxyl groups should be able to explain the 2 extremes of toxic effects for PU-1 and PU-7. Hence, our findings stress the importance of the surface oxygen content and, more importantly, the distribution pattern of different O-containing groups for the cytotoxicity of aged PU particles.

Conclusions

After emission, pristine air particles are subjected to significant attack under different atmospheric conditions, such as profound ageing upon interaction with trace gases including SO₂, O₃ and NO_x, giving rise to remarkable alterations in physicochemical properties. Despite numerous toxicity studies on fine air particles, rather limited knowledge has been obtained regarding ageing-determined toxicity changes. To fill in these knowledge gaps, in this study, we simulated the environmental ageing process using CB particles as a model for real PM, and we specifically inspected the differential toxicity effects of aged CB towards susceptible cells. Our data revealed that the O-content and the distribution pattern of surface O-containing groups essentially dictated the bioreactivity and cytocompatibility of aged CB particles towards cells. While surface properties have been demonstrated to influence the cytotoxicity profiles of nanomaterials, most attention has been paid to interpreting how an increase in O-functionalities affects the colloidal stability, zeta potential and interactions with cells.^{54–56} In contrast to previous studies, the current study has garnered new insights into the physicochemical determinants of CB-induced cytotoxicity; the proportion of O-containing groups (such as ample epoxy and hydroxyl groups) is a crucial variable.

Additionally, with the rapid increase in production and applications of carbonaceous nanomaterials (*i.e.* graphene and its derivatives, carbon nanotubes and fullerenes), their accidental release into the environment is inevitable.^{57–59} Similarly to air particles, once they enter environmental media, carbonaceous nanomaterials undergo diverse transformation processes, leading to significant alterations of their physicochemical properties and, consequently, their biosafety profiles. Hence, the findings from the current study

will have important implications for bio-risk assessments of carbon-based nanomaterials. Taken together, this study unearthed the significance of ageing in altering particle toxicity and also shed light on the importance of O-containing groups when considering cytotoxicity-associated physicochemical determinants.

Conflicts of interest

The authors declare no competing financial interest.

Acknowledgements

This work was supported by grants from the National Natural Science Foundation of China (grant numbers: 21637004, 91943301, 21906175 and 21920102007), the Beijing Natural Science Foundation (grant numbers: 8191002 and 8204071) and the international collaboration key grant from the Chinese Academy of Sciences (grant number: 121311KYSB20190010). We thank Dr. Jie Shao and Dr. Zhiguo Sheng for reagents and helpful discussion.

References

- 1 J. Lelieveld, J. S. Evans, M. Fnais, D. Giannadaki and A. Pozzer, The contribution of outdoor air pollution sources to premature mortality on a global scale, *Nature*, 2015, **525**, 367–371.
- 2 R. Beelen, O. Raaschou-Nielsen, M. Stafoggia, Z. J. Andersen, G. Weinmayr, B. Hoffmann, K. Wolf, E. Samoli, P. Fischer, M. Nieuwenhuijsen, P. Vineis, W. W. Xun, K. Katsouyanni, K. Dimakopoulou, A. Oudin, B. Forsberg, L. Modig, A. S. Havulinna, T. Lanki, A. Turunen, B. Oftedal, W. Nystad, P. Nafstad, U. De Faire, N. L. Pedersen, C. G. Ostenson, L. Fratiglioni, J. Penell, M. Korek, G. Pershagen, K. T. Eriksen, K. Overvad, T. Ellermann, M. Eeftens, P. H. Peeters, K. Meliefste, M. Wang, B. Bueno-de-Mesquita, D. Sugiri, U. Kramer, J. Heinrich, K. de Hoogh, T. Key, A. Peters, R. Hampel, H. Concin, G. Nagel, A. Ineichen, E. Schaffner, N. Probst-Hensch, N. Kunzli, C. Schindler, T. Schikowski, M. Adam, H. Phuleria, A. Vilier, F. Clavel-Chapelon, C. Declercq, S. Grioni, V. Krogh, M. Y. Tsai, F. Ricceri, C. Sacerdote, C. Galassi, E. Migliore, A. Ranzi, G. Cesaroni, C. Badaloni, F. Forastiere, I. Tamayo, P. Amiano, M. Dorronsoro, M. Katsoulis, A. Trichopoulou, B. Brunekreef and G. Hoek, Effects of long-term exposure to air pollution on natural-cause mortality: an analysis of 22 European cohorts within the multicentre ESCAPE project, *Lancet*, 2014, **383**, 785–795.
- 3 A. Valavanidis, K. Fiotakis and T. Vlachogianni, Airborne particulate matter and human health: toxicological assessment and importance of size and composition of particles for oxidative damage and carcinogenic mechanisms, *J. Environ. Sci. Health, Part C: Environ. Carcinog. Ecotoxicol. Rev.*, 2008, **26**, 339–362.
- 4 Z. Meng, D. Dabdub and J. J. S. Seinfeld, Chemical coupling between atmospheric ozone and particulate matter, *Science*, 1997, **277**, 116–119.

- 5 C. Heald and J. J. S. A. Kroll, The fuel of atmospheric chemistry: toward a complete description of reactive organic carbon, *Sci. Adv.*, 2020, **6**, eaay8967.
- 6 Y. Zhao, Y. Liu, J. Ma, Q. Ma and H. J. A. E. He, Heterogeneous reaction of SO₂ with soot: the roles of relative humidity and surface composition of soot in surface sulfate formation, *Atmos. Environ.*, 2017, **152**, 465–476.
- 7 B. C. Peebles, P. K. Dutta, W. J. Waldman, F. A. Villamena, K. Nash, M. Severance and A. Nagy, Physicochemical and toxicological properties of commercial carbon blacks modified by reaction with ozone, *Environ. Sci. Technol.*, 2011, **45**, 10668–10675.
- 8 Q. Li, J. Shang, J. Liu, W. Xu, X. Feng, R. Li and T. Zhu, Physicochemical characteristics, oxidative capacities and cytotoxicities of sulfate-coated, 1,4-NQ-coated and ozone-aged black carbon particles, *Atmos. Res.*, 2015, **153**, 535–542.
- 9 H. Jiang, Y. Liu, Y. Xie, J. Liu, T. Chen, Q. Ma and H. He, Oxidation potential reduction of carbon nanomaterials during atmospheric-relevant aging: role of surface coating, *Environ. Sci. Technol.*, 2019, **53**, 10454–10461.
- 10 R. Zhang, A. F. Khalizov, J. Pagels, D. Zhang, H. Xue and P. H. McMurry, Variability in morphology, hygroscopicity, and optical properties of soot aerosols during atmospheric processing, *Proc. Natl. Acad. Sci. U. S. A.*, 2008, **105**, 10291–10296.
- 11 C. Han, Y. Liu, J. Ma and H. He, Key role of organic carbon in the sunlight-enhanced atmospheric aging of soot by O₂, *Proc. Natl. Acad. Sci. U. S. A.*, 2012, **109**, 21250–21255.
- 12 M. E. Monge, B. D'Anna, L. Mazri, A. Giroir-Fendler, M. Ammann, D. J. Donaldson and C. George, Light changes the atmospheric reactivity of soot, *Proc. Natl. Acad. Sci. U. S. A.*, 2010, **107**, 6605–6609.
- 13 W. R. Cofer, D. R. Schryer and R. S. Rogowski, The oxidation of SO₂ on carbon particles in the presence of O₃, NO₂ and N₂O, *Atmos. Environ.*, 1981, **15**, 1281–1286.
- 14 Y. Zhang, S. Tong, M. Ge, B. Jing, S. Hou, F. Tan, Y. Chen, Y. Guo and L. Wu, The influence of relative humidity on the heterogeneous oxidation of sulfur dioxide by ozone on calcium carbonate particles, *Sci. Total Environ.*, 2018, **633**, 1253–1262.
- 15 S. Philip, R. V. Martin, A. van Donkelaar, J. W. Lo, Y. Wang, D. Chen, L. Zhang, P. S. Kasibhatla, S. Wang, Q. Zhang, Z. Lu, D. G. Streets, S. Bittman and D. J. Macdonald, Global chemical composition of ambient fine particulate matter for exposure assessment, *Environ. Sci. Technol.*, 2014, **48**, 13060–13068.
- 16 Y. Sun, Q. Zhang, M. Zheng, X. Ding, E. S. Edgerton and X. Wang, Characterization and source apportionment of water-soluble organic matter in atmospheric fine particles (PM_{2.5}) with high-resolution aerosol mass spectrometry and GC-MS, *Environ. Sci. Technol.*, 2011, **45**, 4854–4861.
- 17 J. Ma, A. Guo, S. Wang, S. Man, Y. Zhang, S. Liu and Y. Liu, From the lung to the knee joint: toxicity evaluation of carbon black nanoparticles on macrophages and chondrocytes, *J. Hazard. Mater.*, 2018, **353**, 329–339.
- 18 Q. Ren, Y. Wu, J. Ma, Q. Shan, S. Liu and Y. Liu, Carbon black-induced detrimental effect on osteoblasts at low concentrations: remarkably compromised differentiation without significant cytotoxicity, *Ecotoxicol. Environ. Saf.*, 2019, **178**, 211–220.
- 19 Y. Liu, H. Jiang, C. Liu, Y. Ge, L. Wang, B. Zhang, H. He and S. Liu, Influence of functional groups on toxicity of carbon nanomaterials, *Atmos. Chem. Phys.*, 2019, **19**, 8175–8187.
- 20 C. Kiratipaiboon, T. A. Stueckle, R. Ghosh, L. W. Rojanasakul, Y. C. Chen, C. Z. Dinu and Y. Rojanasakul, Acquisition of cancer stem cell-like properties in human small airway epithelial cells after a long-term exposure to carbon nanomaterials, *Environ. Sci.: Nano*, 2019, **6**, 2152–2170.
- 21 S. Hussain, L. C. Thomassen, I. Ferecatu, M. C. Borot, K. Andreau, J. A. Martens, J. Fleury, A. Baeza-Squiban, F. Marano and S. Boland, Carbon black and titanium dioxide nanoparticles elicit distinct apoptotic pathways in bronchial epithelial cells, *Part. Fibre. Toxicol.*, 2010, **7**, 10.
- 22 P. Jackson, K. S. Hougaard, A. M. Boisen, N. R. Jacobsen, K. A. Jensen, P. Moller, G. Brunborg, K. B. Gutzkow, O. Andersen, S. Loft, U. Vogel and H. Wallin, Pulmonary exposure to carbon black by inhalation or instillation in pregnant mice: effects on liver DNA strand breaks in dams and offspring, *Nanotoxicology*, 2012, **6**, 486–500.
- 23 M. Geiser and W. G. Kreyling, Deposition and biokinetics of inhaled nanoparticles, *Part. Fibre. Toxicol.*, 2010, **7**, 2.
- 24 S. A. MacParland, K. M. Tsoi, B. Ouyang, X. Z. Ma, J. Manuel, A. Fawaz, M. A. Ostrowski, B. A. Alman, A. Zilman, W. C. Chan and I. D. McGilvray, Phenotype determines nanoparticle uptake by human macrophages from liver and blood, *ACS Nano*, 2017, **11**, 2428–2443.
- 25 R. Miyata and S. F. van Eeden, The innate and adaptive immune response induced by alveolar macrophages exposed to ambient particulate matter, *Toxicol. Appl. Pharmacol.*, 2011, **257**, 209–226.
- 26 B. M. Rothen-Rutishauser, S. Schurch, B. Haenni, N. Kapp and P. Gehr, Interaction of fine particles and nanoparticles with red blood cells visualized with advanced microscopic techniques, *Environ. Sci. Technol.*, 2006, **40**, 4353–4359.
- 27 Y. Zhao, X. Sun, G. Zhang, B. G. Trewyn, I. I. Slowing and V. S. Lin, Interaction of mesoporous silica nanoparticles with human red blood cell membranes: size and surface effects, *ACS Nano*, 2011, **5**, 1366–1375.
- 28 C. A. Simpson, A. C. Agrawal, A. Balinski, K. M. Harkness and D. E. Cliffl, Short-chain PEG mixed monolayer protected gold clusters increase clearance and red blood cell counts, *ACS Nano*, 2011, **5**, 3577–3584.
- 29 V. Kodali, M. H. Littke, S. C. Tilton, J. G. Teeguarden, L. Shi, C. W. Frevert, W. Wang, J. G. Pounds and B. D. Thrall, Dysregulation of macrophage activation profiles by engineered nanoparticles, *ACS Nano*, 2013, **7**, 6997–7010.
- 30 D. Wang, L. Zhu, J. F. Chen and L. Dai, Can graphene quantum dots cause DNA damage in cells?, *Nanoscale*, 2015, **7**, 9894–9901.
- 31 Y. Xu, S. Y. Wang, J. Yang, X. Gu, J. Zhang, Y. F. Zheng, J. Yang, L. Xu and X. Q. Zhu, Multiwall carbon nano-onions induce DNA damage and apoptosis in human umbilical vein endothelial cells, *Environ. Toxicol.*, 2013, **28**, 442–450.

- 32 L. Xu, Y. Dai, Z. Wang, J. Zhao, F. Li, J. C. White and B. Xing, Graphene quantum dots in alveolar macrophage: uptake-exocytosis, accumulation in nuclei, nuclear responses and DNA cleavage, *Part. Fibre. Toxicol.*, 2018, **15**, 45.
- 33 H. Jiang, Y. Xie, Y. Ge, H. He and Y. Liu, Effects of ultrasonic treatment on dithiothreitol (DTT) assay measurements for carbon materials, *J. Environ. Sci.*, 2019, **84**, 51–58.
- 34 Q. Li, J. Shang and T. Zhu, Physicochemical characteristics and toxic effects of ozone-oxidized black carbon particles, *Atmos. Environ.*, 2013, **81**, 68–75.
- 35 T. Du, A. S. Adeleye, T. Zhang, N. Yang, R. Hao, Y. Li, W. Song and W. Chen, Effects of ozone and produced hydroxyl radicals on the transformation of graphene oxide in aqueous media, *Environ. Sci.: Nano*, 2019, **6**, 2484–2494.
- 36 M. Yang, K. Flavin, I. Kopf, G. Radics, C. H. Hearnden, G. J. McManus, B. Moran, A. Villalta-Cerdas, L. A. Echegoyen and S. Giordani, Functionalization of carbon nanoparticles modulates inflammatory cell recruitment and NLRP3 inflammasome activation, *Small*, 2013, **9**, 4194–4206.
- 37 K. Yang, Y. Li, X. Tan, R. Peng and Z. Liu, Behavior and toxicity of graphene and its functionalized derivatives in biological systems, *Small*, 2013, **9**, 1492–1503.
- 38 G. Sigmund, C. Jiang, T. Hofmann and W. Chen, Environmental transformation of natural and engineered carbon nanoparticles and implications for the fate of organic contaminants, *Environ. Sci.: Nano*, 2018, **5**, 2500–2518.
- 39 R. Li, L. M. Guiney, C. H. Chang, N. D. Mansukhani, Z. Ji, X. Wang, Y. Liao, W. Jiang, B. Sun and M. C. Hersam, Surface oxidation of graphene oxide determines membrane damage, lipid peroxidation, and cytotoxicity in macrophages in a pulmonary toxicity model, *ACS Nano*, 2018, **12**, 1390–1402.
- 40 Y. Wu, Y. Guo, H. Song, W. Liu, Y. Yang, Y. Liu, N. Sang, Y. Y. Zuo and S. Liu, Oxygen content determines the bio-reactivity and toxicity profiles of carbon black particles, *Ecotoxicol. Environ. Saf.*, 2018, **150**, 207–214.
- 41 Z. Wang, S. Liu, J. Ma, G. Qu, X. Wang, S. Yu, J. He, J. Liu, T. Xia and G. Jiang, Silver nanoparticles induced RNA polymerase-silver binding and RNA transcription inhibition in erythroid progenitor cells, *ACS Nano*, 2013, **7**, 4171–4186.
- 42 L. Gutierrez, N. Caballero, L. Fernandez-Calleja, E. Karkoulia and J. Strouboulis, Regulation of GATA1 levels in erythropoiesis, *IUBMB Life*, 2020, **72**, 89–105.
- 43 J. J. Welch, J. A. Watts, C. R. Vakoc, Y. Yao, H. Wang, R. C. Hardison, G. A. Blobel, L. A. Chodosh and M. J. Weiss, Global regulation of erythroid gene expression by transcription factor GATA-1, *Blood*, 2004, **104**, 3136–3147.
- 44 R. A. Shivdasani and S. H. Orkin, Erythropoiesis and globin gene expression in mice lacking the transcription factor NF-E2, *Proc. Natl. Acad. Sci. U. S. A.*, 1995, **92**, 8690–8694.
- 45 M. Mutschler, A. S. Magin, M. Buerge, R. Roelz, D. H. Schanne, B. Will, I. H. Pilz, A. R. Migliaccio and H. L. Pahl, NF-E2 overexpression delays erythroid maturation and increases erythrocyte production, *Br. J. Haematol.*, 2009, **146**, 203–217.
- 46 E. Ingley, P. A. Tilbrook and S. P. Klinken, New insights into the regulation of erythroid cells, *IUBMB Life*, 2004, **56**, 177–184.
- 47 M. I. Khan, A. Mohammad, G. Patil, S. A. Naqvi, L. K. Chauhan and I. Ahmad, Induction of ROS, mitochondrial damage and autophagy in lung epithelial cancer cells by iron oxide nanoparticles, *Biomaterials*, 2012, **33**, 1477–1488.
- 48 X. Jin, B. Xue, Q. Zhou, R. Su and Z. Li, Mitochondrial damage mediated by ROS incurs bronchial epithelial cell apoptosis upon ambient PM_{2.5} exposure, *J. Toxicol. Sci.*, 2018, **43**, 101–111.
- 49 Y. N. Qiu, G. H. Wang, F. Zhou, J. J. Hao, L. Tian, L. F. Guan, X. K. Geng, Y. C. Ding, H. W. Wu and K. Z. Zhang, PM_{2.5} induces liver fibrosis via triggering ROS-mediated mitophagy, *Ecotoxicol. Environ. Saf.*, 2019, **167**, 178–187.
- 50 A. Sharma, K. Singh and A. Almasan, Histone H2AX phosphorylation: a marker for DNA damage, *Methods Mol. Biol.*, 2012, **920**, 613–626.
- 51 A. L. Holder, B. J. Carter, R. Goth-Goldstein, D. Lucas and C. P. Koshland, Increased cytotoxicity of oxidized flame soot, *Atmos. Pollut. Res.*, 2012, **3**, 25–31.
- 52 Y. Liu, J. Liggio, S. M. Li, D. Breznan, R. Vincent, E. M. Thomson, P. Kumarathasan, D. Das, J. Abbatt, M. Antinolo and L. Russell, Chemical and toxicological evolution of carbon nanotubes during atmospherically relevant aging processes, *Environ. Sci. Technol.*, 2015, **49**, 2806–2814.
- 53 A. Magrez, S. Kasas, V. Salicio, N. Pasquier, J. W. Seo, M. Celio, S. Catsicas, B. Schwaller and L. Forro, Cellular toxicity of carbon-based nanomaterials, *Nano Lett.*, 2006, **6**, 1121–1125.
- 54 Y. Qi, Y. Liu, T. Xia, A. Xu, S. Liu and W. Chen, The biotransformation of graphene oxide in lung fluids significantly alters its inherent properties and bioactivities toward immune cells, *NPG Asia Mater.*, 2018, **10**, 385–396.
- 55 M. Xu, J. Zhu, F. Wang, Y. Xiong, Y. Wu, Q. Wang, J. Weng, Z. Zhang, W. Chen and S. Liu, Improved *in vitro* and *in vivo* biocompatibility of graphene oxide through surface modification: poly (acrylic acid)-functionalization is superior to PEGylation, *ACS Nano*, 2016, **10**, 3267–3281.
- 56 J. Zhu, M. Xu, M. Gao, Z. Zhang, Y. Xu, T. Xia and S. Liu, Graphene oxide induced perturbation to plasma membrane and cytoskeletal meshwork sensitize cancer cells to chemotherapeutic agents, *ACS Nano*, 2017, **11**, 2637–2651.
- 57 S. Liu, Y. Lu and W. Chen, Bridge knowledge gaps in environmental health and safety for sustainable development of nano-industries, *Nano Today*, 2018, **23**, 11–15.
- 58 A. S. Adeleye, J. R. Conway, K. Garner, Y. Huang, Y. Su and A. A. Keller, Engineered nanomaterials for water treatment and remediation: costs, benefits, and applicability, *Chem. Eng. J.*, 2016, **286**, 640–662.
- 59 K. Krishnamoorthy, K. Jeyasubramanian, M. Premanathan, G. Subbiah, H. S. Shin and S. J. Kim, Graphene oxide nanopaint, *Carbon*, 2014, **72**, 328–337.